We are IntechOpen, the world's leading publisher of Open Access books Built by scientists, for scientists

6,900
Open access books available

185,000
International authors and editors

200M
Downloads

Our authors are among the

154
Countries delivered to

TOP 1%
most cited scientists

12.2%
Contributors from top 500 universities



WEB OF SCIENCE™

Selection of our books indexed in the Book Citation Index in Web of Science™ Core Collection (BKCI)

Interested in publishing with us?
Contact book.department@intechopen.com

Numbers displayed above are based on latest data collected.
For more information visit www.intechopen.com



Chapter

Far-Red Light Absorbing Photosynthetic Pigments in Cyanobacteria: Steady-State Fluorescence Detection, Time-Resolved Fluorescence Spectroscopy, and Confocal Laser Scanning Microscopy

Svetlana Averina, Ekaterina Senatskaya and Alexander Pinevich

Abstract

The use of far-red light (FRL) is observed in some cyanobacteria, as well as in some marine and freshwater algae. While algae mobilize FRL absorbing antenna, which contains common chlorophyll *a* (Chl *a*), cyanobacteria produce red-shifted Chl *d* and/or Chl *f*. These pigments are synthesized either irrespective of ambient light or synthesized during FRL photoacclimation (FaRLiP), or adaptive remodeling of photosynthetic apparatus induced by relative enrichment with FRL quanta. The presence of red-shifted chlorophylls as well as their functions and topography are registered with various methods based on fluorescence measurement, such as: (1) steady-state fluorescence detection in live cells, cell fractions, and photosynthetic apparatus constituents; (2) time-resolved fluorescence spectroscopy, which traces energy transfer between individual pigments; (3) confocal laser scanning microscopy (CLSM), which helps to localize photosynthetic pigments in situ. This chapter describes photosynthetic apparatus in cyanobacteria and their photoacclimation phenomena. Over past decades, FRL photoacclimation has been studied in a small number of cyanobacteria. Novel Chl *f*-producing strains *Chlorogloeopsis* sp. CALU 759 and *Synechocystis* sp. CALU 1173 would represent promising model objects. Importantly, although they belong to alternative morphotypes and distant phylogenetic lineages, fluorescence pattern of their FRL-grown cells similarly falls within general FaRLiP response.

Keywords: cyanobacteria, chlorophylls *d* and *f*, steady-state fluorescence detection, time-resolved fluorescence spectroscopy, confocal laser scanning microscopy

1. Introduction

Cyanobacteria are the only up-to-date known prokaryotes capable of oxygenic photosynthesis. They assimilate light energy via electron transfer from water to oxidized ferredoxin, and excrete triplet dioxygen as a waste product. The majority of cyanobacteria possess chlorophyll *a* (Chl *a*), bicyclic carotenoids, and phycobiliproteins (PBP). In common, these pigments absorb light quanta within a whole visible area (400–700 nm). At the same time, some cyanobacteria have been shown to use far-red light (FRL) with wavelengths of more than 700 nm [1]. For this purpose, red-shifted Chl *d* and/or Chl *f* are produced [2, 3]. In search of novel representatives of FRL-adapting cyanobacteria, various analytical methods are employed, especially those based on fluorescence detection.

This chapter includes four sections, which describe: photosynthetic apparatus in cyanobacteria; photoacclimation phenomena in cyanobacteria; fluorescence methods employed in the study of FRL-adapting cyanobacteria; FRL photoacclimating strains in CALU collection (St. Petersburg University, St. Petersburg, Russia).

2. Photosynthetic apparatus in cyanobacteria

Light energy assimilation machinery in cyanobacteria is usually localized in/on intracytoplasmic membrane structures termed thylakoids. Among principal constituents are: reaction centers (RC) of two photosystems (PSs), a main light-harvesting complex (LHC), and electron transfer chain (ETC). The essential component of PSII is unique light-dependent enzyme—H_2O dehydrogenase, or water oxidizing complex (WOC).

In the majority of cyanobacteria, Chl *a* represents the only chlorophyll while in rare cases other chlorophylls are additionally produced [4, 5].

Both PSs are supplied with their respective light-harvesting antennae, which contain Chl *a*. LHC is usually represented by phycobilisome (PBS), supramolecular aggregate of phycobiliproteins (PBP) stabilized by colorless linker polypeptides, and anchored to thylakoid surface with high-molecular mass colored polypeptide [6, 7]. PBP apoprotein moiety is represented by α or β subunits that covalently bind non-porphyrin tetrapyrrole chromophores [8, 9]. Depending on chromophore type and number, four main PBP types are distinguished: phycocyanin (PC), phycoerythrin (PE), allophycocyanin (APC), and phycoerythrocyanin (PEC) [8]. Standard PBS consists of the central core and peripheral rods. The former contains two to three "cylinders" assembled of several $(\alpha\beta)_3$ trimers each, while the latter includes several $[2(\alpha\beta)_3]$ hexamers each. Due to anisotropic structure of rods and core, a waste-less channeling of excitation energy to RC chlorophyll is achieved [10, 11].

3. Photoacclimation phenomena in cyanobacteria

Cyanobacteria can acclimate themselves to light quantity and quality, that is, they adaptively respond to the shifts in ambient light color and intensity. For this purpose, they can modulate: (1) PS content, (2) the interaction between PS and PBS, and (3) LHC structure, PBP content in particular.

In the first case, antenna size varies inversely with a flood of light quanta. This strategy is performed via the changes in thylakoid surface and PS packing density [12].

In the second case (given that ambient light is enriched with either short- or long-wavelength quanta), excitation energy equally distributes between long-wavelength PSI and short-wavelength PSII. This phenomenon is termed State 1 ↔ State 2 transition. State 1 is achieved in response to relative over-excitation of PSII [13]. Here, PBS behaves as a mobile antenna, and it laterally moves from PSII to PSI. In the opposite situation (State 2), PBS detaches from PSI and comes back to PSII [14]. State transition scenario is as follows: up- or downshifts in ETC reduction level → redox-sensitive (de)phosphorylation of proteins within the PBS baseplate → coulomb attraction/repulsion between PBS and PS [15].

In the third case, PBS absorbance peak adjusts to ambient light color (preferentially green or red). This adaptation is performed via the shifts in PE (green light absorbing PBP) and PC (red light absorbing PBP) content. The knowledge on this phenomenon termed complementary chromatic adaptation (CA) has been comprehensively reviewed [16, 17].

In agreement with a response to green or red light, cyanobacteria have been ascribed to three CA groups [18]: group CA1 (steady PE and PC content), group CA2 (PE content varies), and group CA3 (PE and PC contents vary).

Groups CA2 and CA3 are specified according to the presence of regulatory photoreceptors CcaS and RcaE, which belong to the "cyanobacteriochromes" phytochrome family [19–21]. These receptors contain one and the same bilin-binding domain GAF (cyclic guanosine monophosphate phosphodiesterase/adenylyl cyclase/FhlA), which regulates green or red light-triggered photocycle [22, 23]. In the case of CA2, under green light, CcaS (signal transducer) phosphorylates transcription factor CcaR (response regulator) that induces the production of PE [22]. In the case of CA3, under red light, RcaE phosphorylates transcription factors RcaF and RcaC, which regulate numerous participants of PC and PE biosynthesis pathway [23, 24].

Group CA4 is represented by marine *Synechococcus* strains grown under blue or green light [25–27]. Under blue light, PE phycoerythrobilin chromophores replace phycourobilin chromophores, which adapt PBS to the use of smaller wavelength light. Although corresponding photoreceptor is unknown, light signal was shown to be transmitted to transcription factors FciA and FciB with a participation of chromophore liases MpeZ and MpeW [26, 28].

Group CA5 is typical of *Acaryochloris marina* [29]. Irrespective of light conditions, this cyanobacterium uses membrane-embedded LHC containing Chl *d*. Under red light (625 nm), atypical rod-like PC and APC containing PBS is additionally produced [30]. Such PBS disassembled in far-red light (720 nm), and corresponding PBP are destroyed [31, 32]. In other words, in these light conditions, *A. marina* uses two LHCs in common. Although the underlying regulatory mechanism is unknown, *A. marina* genome has been shown to contain a motif similar to that coding for FRL accepting phytochromes [33].

Group CA6 is represented by several strains of cyanobacteria, which adaptively produce Chl *f* and/or Chl *d* in FRL [16]. In more detail, this phenomenon is dwelled on below.

Group CA7 [16] has been described in the case of cyanobacteria which synthesize yellow-green light absorbing PEC, and regulate the amount of this PBP light dependently. Similar to CA2, the adaptive response is under control of two-component regulatory system CcaS/CcaR.

Another type of reaction to green or red light is typical for CA0 group [16]. In this case, PBP content is stable, while the amount of CpcG2 (CpcL) and CpcG1 linker polypeptides varies reciprocally [34]. In green light, the CcaS/CcaR system upgrades the production of CpcG2 (CpcL) linker involved in the biogenesis of APC

lacking PBS [22]. The CpcG2 (CpcL) type PBS is suggested to be rod-like, and it possibly supplies energy to PSI under suboptimal conditions [16, 22].

Cyanobacterial response to FRL has been described in cyanobacteria only recently, and it is based on red-shifted Chl *d* and/or Chl *f* (697 and 706 nm maxima in methanol, respectively). First representative of Chl *d*-containing species was *A. marina* [1], while the initially described Chl *f*-containing species was *Halomicronema hongdechloris* [35].

Cyanobacteria can use two main strategies of FRL photoacclimation.

In the first strategy, Chl *d* represents the bulk chlorophyll, and it is constitutively produced in *A. marina* [36–39]. The pigment participates in PSI and PSII, as well as in LHC [40–43]. Such strategy is observed in cyanobacteria inhabiting marine or continental haline water bodies poor in visible light but rich in FRL.

In the second strategy, Chl *a* represents the bulk chlorophyll while Chl *f* (sometimes together with a small amount of Chl *d*) is produced adaptively in FRL [35, 44–46]. In this case, ~10% of Chl *a* in PSI and PSII is replaced with Chl *f*; special paralogue polypeptides substitute for PSI and PSII subunits; PBS is remodeled [45]. The latter strategy is termed FRL photoacclimation—FaRLiP [3], or CA6 (see above). In this strategy, FRL induces the expression of 21 genes of FaRLiP cluster including those coding for PSI and PSII subunit paralogues [2, 45, 46]. The products of these genes specifically bind Chl *a* together with red-shifted chlorophylls [2]. FaRLiP cluster also includes the genes coding for PBP subunit paralogues [45, 47]. Resulting PBS are optimal in new light climate because they are devoid of short-wavelength PBP (PE and PEC), and correspondingly lack rod periphery [46].

Leptolyngbya sp. JSC-1 grown in white light (WL) or red light (RL) contains the standard five-cylinder-core PBS, while in FRL a two-cylinder-core PBS is produced [45]. The latter has a 708-nm maximum (40 nm longer than in APCB, the top wavelength PBP previously reported). In its turn, FRL-grown *H. hongdechloris* produces a two-cylinder-core mini PBS, which contains APC with 653- and 712-nm maxima [48].

FRL-grown *Synechococcus* sp. PCC 7335 produces PBS of two types: three-cylinder-core PBS containing PC and APC, and two-cylinder-core PBS, which contains only APC with FaRLiP gene encoded subunits, and displays red-shifted 650- and 711-nm light absorbance and 730-nm fluorescence emission maxima [49].

FaRLiP response falls under the control of two-component phosphorelay system [47]. Sensory component (RfpA photoreceptor) represents a far-red light regulated cyanobacteriochrome with histidine kinase domain. Response regulators RfpB and RfpC have two CheY-like signal accepting domains, which flank the DNA-binding domain. RfpB acts as a transcription activator for FaRLiP genes [47, 50]. Within this phoshorelay, RfpA histidine kinase becomes (de)activated, and that influences the RfpB key response regulator. In its turn, RfpC is involved in transfer of phosphoryl group from RfpA to RfpB.

4. Fluorescence methods employed in the research of far-red light-adapting cyanobacteria

4.1 Steady-state fluorescence detection

Absorbed energy of light quanta brings photosynthetic pigments into excited state, which is relaxed by: (1) productive energy assimilation in the form of charge separation within RC, (2) counterproductive energy dissipation into heat, or with fluorescence quanta [51]. Since the photosynthetic apparatus is less than 100%

effective, the second mechanism is universally in action, although it depends on environmental and physiological regimes.

Steady-state fluorescence detection helps to identify photosynthetic pigments because they demonstrate individual fluorescence excitation and emission spectra. Additionally, this method can detect energy transfer between pigments. Fluorescence spectra can be obtained at either room or cryogenic temperature (most frequently, 77 K). Low temperatures are preferred because of lowered molecular mobility, and due to smaller intramolecular vibrations; as a result, peaks become higher and better resolved [51]. Importantly, low-temperature regime (4–77 K) helps to discriminate PSI chlorophyll (~ 720 nm) and PSII chlorophyll (~ 685 nm) emission peaks [51–53].

Current data on steady-state fluorescence of red-shifted chlorophylls are few. For instance, the spectra of WL-grown *H. hongdechloris* were compared with those of FRL culture [35]. In the case of WL cells, Chl *a*-specific 405-nm fluorescence excitation yielded fluorescence emission maxima at 640, 658, 682, and 730 nm of comparable height. In contrast, FRL cells exhibited a major 748-nm maximum (indicating the adaptive synthesis of red-shifted Chl *f*), and 682- and 720-nm minor maxima, respectively. Also, the emission at 440-nm excitation was compared in *Calothrix* sp. PCC 7507, *Chlorogloeopsis* sp. PCC 9212, *Chroococcidiopsis* sp. PCC 7203, *Fischerella* sp. PCC 7521, and *Synechococcus* sp. PCC 7335 grown under different light conditions [46]. In all these strains, WL cultures showed emission maxima of Chl *a* (683–684 nm, 693–695 nm, and 718–727 nm). At the same time, FRL spectra were strain specific, Chl *f* being most pronounced (*Calothrix* sp. PCC 7507—736 nm; *Chlorogloeopsis* sp. PCC 9212—739 nm; *Chroococcidiopsis* sp. PCC 7203—718, 736, and 750 nm; *Fischerella* sp. PCC 7521—749 nm; *Synechococcus* sp. PCC 7335—738 nm).

Apart from the experiments on cell suspensions, steady-state fluorescence of Chl *a* and Chl *f* has been detected with subcellular fractions, as well as with PSI, PSII, and PBS preparations. For example, *H. hongdechloris* emission was compared for WL and FRL thylakoid preparations [54]. In WL preparation, major 710-nm peak as well as 680- and 732-nm minor peaks were observed, while FRL preparation demonstrated a major 740-nm peak due to adaptively produced Chl *f*.

Cryogenic detection helped to monitor energy transfer in FRL-adapted *Synechococcus* sp. PCC 7335 [55]. Purified PSI or PSII preparations obtained from FRL-adapted cells showed one and the same well-expressed peak at 738–740 nm indicating similar effectiveness of energy coupling notwithstanding a distinction in PS structure.

Steady-state fluorescence emission was also detected in the experiments with PBP-specific 590-nm excitation of RL- or FRL-grown *Synechococcus* sp. PCC 7335. Besides 643-, 658-, and 679-nm peaks in the RL culture, FRL-grown cells acquired 717- and 737-nm maxima that could be explained by PBS rearrangement due to induction of FaRLiP gene cluster [50].

4.2 Time-resolved fluorescence spectroscopy

The method helps to analyze molecular processes within a picosecond/nanosecond timescale [56]. Because primary photosynthetic processes take several femtoseconds/nanoseconds, time-resolved fluorescence spectroscopy can trace corresponding rates and pathways of energy transfer [57]. Recently, this method has helped to elucidate the role(s) of red-shifted chlorophylls in cyanobacterial PS.

In the case of Chl *f*-producing *H. hongdechloris*, time-resolved fluorescence detection was performed at 77 K, with 425-nm excitation [41]. In WL cells, the excitation raised 685-nm (F685) and 730-nm (F730) emission peaks characteristic

for PSII and PSI correspondingly. A shift from F685 to F695 occurred with time, and an extra F742 peak appeared and decayed. In FRL cells, F685 and F748 maxima were observed. The former quenched rapidly indicating energy transfer from PSII to PSI. F748 signified the presence of Chl *f*, and uphill energy transfer (from Chl *f* to Chl *a*) was proposed.

Time-resolved fluorescence detection within a picosecond/femtosecond timescale was also performed with *H. hongdechloris* thylakoid membrane preparations [54]. Similar to WL cells, WL membrane emission belonged to PSI and PSII Chl *a* (727 and 685 nm correspondingly). However, these peaks were attended with PBP-specific 678-nm peak. In the case of FRL membrane, main fluorescence emission maxima belonged to Chl *a* (685 nm) and Chl *f* (745 nm). In FRL membrane preparations, fluorescence rise and decay curves suggested Chl *f* to be energy donor to Chl *a*.

Later, the reality of uphill energy transfer from Chl *f H. hongdechloris* was confirmed in the experiments using TCSPC (time-correlated single photon counting) and DAS (decay-associated spectra) methods [58]. According to obtained data, energy was transferred within PSII on the route: PBS → Chl *f* → Chl *a*; only then charge separation began, and Chl *a* represented the P680 primary donor. Thus, Chl *f* in *H. hongdechloris* is PSII antenna pigment, and it does not participate in charge separation.

At the same time, the involvement of red-shifted chlorophylls in charge separation within PSI and PSII was proposed for *Chroococcidiopsis* sp. PCC 7203, which adaptively produces Chl *d* and Chl *f* [59, 60]. Data obtained using plenty of methods, TCSPC in particular, showed that RCI in the FRL-adapted cells contained 7–8 Chl *f* molecules, together with 90 Chl *a* molecules. Special pair (P_A and P_B) was represented by Chl *a* and Chl *a* epimer (*a′*). Primary acceptors (A_{0A} and A_{0B}) were also Chl *a* molecules. Chl *f* molecule absorbing 745-nm light was associated with primary donor (A_{-1A} and/or A_{-1B}). In its turn, RCII contained 4 Chl *f* molecules, 1 Chl *d* molecule, and 30 Chl *a* molecules. Primary donors (Chl_{D1}) were either Chl *d* or Chl *f* molecules absorbing 727-nm light.

Room temperature and 77 K fluorescence data in unicellular strain KC1 producing Chl *f* in FRL helped to obtain TRS (time-resolved) and DAS (decay-associated) emission spectra [61]. In the experiments with PSI exited with 405-nm laser, energy was rapidly transferred to Chl *f* (emission maxima 720–760 and 805 nm). In the case of 630-nm excitation (light absorbed by PBP associated with PSII), energy was transferred to Chl *f* (emission maxima 720–770 and 810 nm) and Chl *a* (emission maximum 694 nm). Distinctions in Chl *f* fluorescence show that PSI and PSII contained Chl *f* molecules with different properties, and possibly they represented antenna pigments.

Similarly, femtosecond pump-probe spectroscopy of *Fischerella thermalis* PCC 7521 [62] showed that Chl *f* represented PSI antenna pigment; it was also argued that energy was transferred uphill from Chl *f* to P700 Chl *a* special pair.

Time-resolved fluorescence spectroscopy also helped to analyze energy transfer in RL-or FRL-grown cells of *Synechococcus* sp. PCC 7335 [55], as well as in *A. marina* mini PBS [63].

4.3 Confocal laser scanning microscopy (CLSM)

The method is based on the auto fluorescence of photosynthetic pigments, chlorophylls in the first instance [64]. CLSM permits to distinguish individual pigments based on their emission peaks, to evaluate peak intensity, and to localize pigments in situ. Highly sensitive up-to-date CLSM microscopes help to obtain 3D images of

cells and tissues, and to analyze dynamic physiological processes. Unfortunately, the potentiality of this method, at least with regard to FRL-adapting cyanobacteria, is underestimated, and thus corresponding data are few.

CLSM has been applied to the study of Chl *d* and PBP localization in *Candidatus* Acaryochloris bahamensis, an epibiont of colonial ascidian *Lissoclinum fragile* [65]. In 3D reconstruction, these pigments were asymmetrically distributed throughout cell interior and that possibly promoted optimal sunlight absorption within *L. fragile* tunic. *Acaryochloris*-like cells were also shown to inhabit the surface of *Cystodytes dellechiajei* ascidian body, and CLSM data indicated the presence of Chl *d* and PBP in this cyanobacterium [66].

Anisotropic distribution of pigments was also observed in *H. hongdechloris,* which adaptively produces accessory Chl *f* in FRL [67]. In WL culture, chlorophylls and PBP were shown to co-localize at cell periphery. However, in FRL culture, PBP fluorescence was detected only at cell poles. In their turn, FRL-grown *Synechococcus* sp. PCC 7335 demonstrated lower PBP fluorescence and higher chlorophyll fluorescence compared with WL cells. In FRL culture, PBP fluorescence was spatially isolated from chlorophyll fluorescence: the latter occupied cell center indicating that PBS detached from PS.

5. Far-red light photoacclimating strains in the CALU collection

5.1 Growth conditions

An ability of FRL-dependent synthesis of Chl *f* in trichome-forming strain *Chlorogloeopsis* sp. CALU 759 and unicellular strain *Synechocystis* sp. CALU 1173 has been deduced from whole-cell light absorbance spectra (**Figure 1**) as well as according to methanol extract spectrometry and HPLC results.

Liquid cultures were grown for a 2- to 3-week time in modified BG-11 medium [68], at 20–22°C, under permanent WL (500 lx) or FRL illumination (LED with ~750 nm emission maximum).

5.2 Steady-state fluorescence detection protocol

Cell pellet was washed with 100 mM HEPES buffer (pH 8.0), and resuspended in 50 mM HEPES (pH 8.0) with or without the addition of 25% glycerol. Room temperature fluorescence was detected in a Cary Eclipse scanning spectrophotometer/fluorimeter (Agilent Technologies, Santa Clara, CA, USA), and obtained data were treated with a Cary Eclipse Scan program. Emission spectra were detected for excitation at 440 nm (specific for chlorophyll) and 550 nm (specific for PBP). Excitation spectra (chlorophyll fluorescence at 745 nm) were also detected.

5.3 CLSM protocol

The method helped to reveal photosynthetic pigments topography. Life preparations of WL- or FRL-grown cells were observed in a Leica TCS SP5 MP STED confocal microscope (Leica Microsystems GmbH, Germany). Fluorescence was raised with a 458-nm-wavelength nitrogen laser. The images were obtained in XYZ scanning regime with a 0.5-μm step. The following emission channels were used: 560–600 nm (PE), 620–650 nm (PC), 670–700 nm (Chl *a*), and 705/710–790 nm (Chl *f*). The obtained images were analyzed with a LAS AF program.

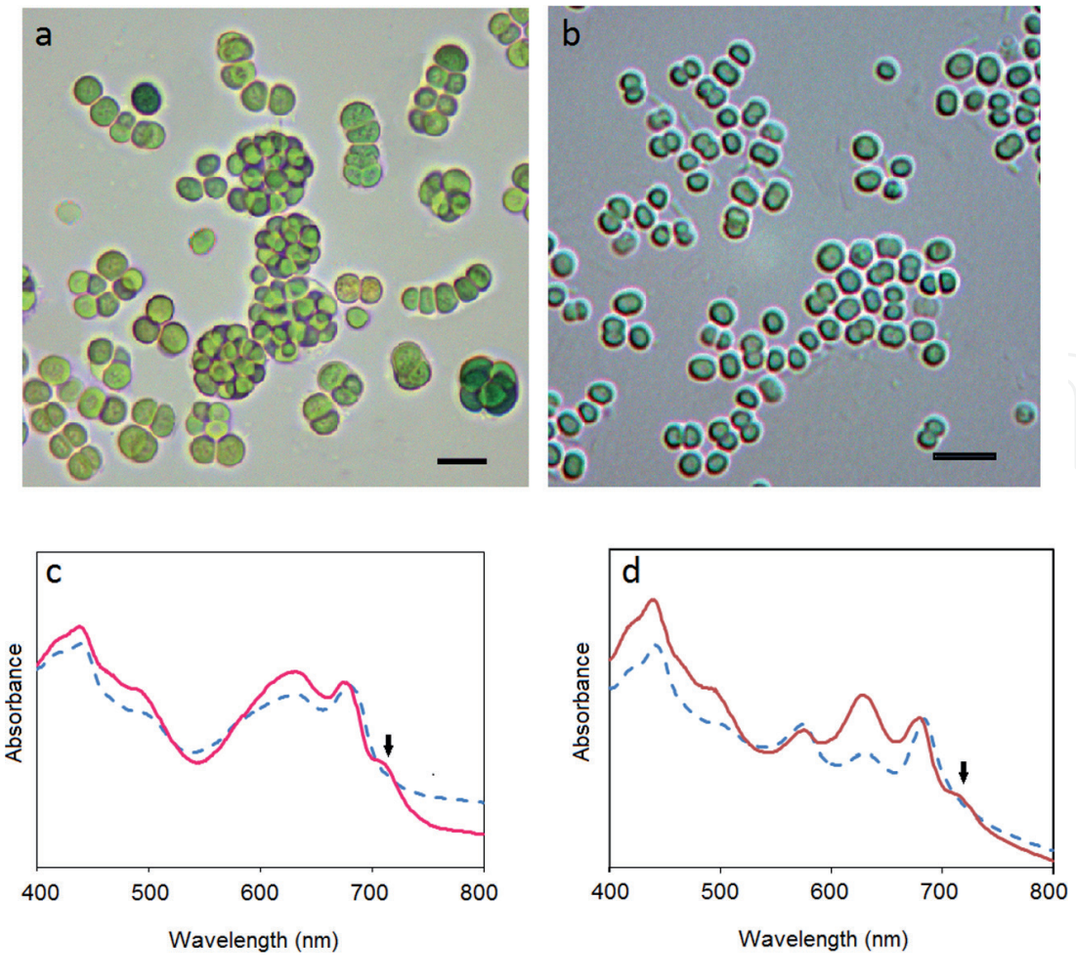


Figure 1.
Light micrographs and light absorbance spectra of Chlorogloeopsis *sp. CALU 759 (a, c) and* Synechocystis *sp. CALU 1173 (b, d) cells. Dashed line, white light-grown cells; solid line, far-red light-grown cells. Arrow, shoulder explained by absorbance of red-shifted chlorophyll. Scale bar, 10 μm (a) or 5 μm (b).*

5.4 Steady-state fluorescence detection of chlorophylls and phycobiliproteins in white light- or far-red light-grown cells

Fluorescence emission spectra (**Figures 2(a,b)** and **3(a,b)**) obtained at chlorophyll-specific 440-nm excitation demonstrated 670–740 nm maxima. In WL-grown *Chlorogloeopsis* sp. CALU 759 (**Figure 2(a)**), it was a single peak with a shoulder while in *Synechocystis* sp. CALU 1173 (**Figure 3(a)**) twin peaks were observed. In FRL-grown cells of both strains, a single 725–740 nm emission peak was observed (**Figures 2(b)** and **3(b)**). In agreement with the previous data obtained with FRL-grown cyanobacteria [35, 46], peaks with more than 720-nm wavelength (observed in light absorbance or fluorescence emission spectra) corresponded to Chl *f*.

Fluorescence emission spectra obtained with PBP-specific 590-nm excitation resulted in 645–660 nm emission peak with broad 690–715 nm shoulder. In WL-grown *Chlorogloeopsis* sp. CALU 759 (**Figure 2(c)**), the shoulder was steep while in *Synechocystis* sp. CALU 1173 (**Figure 3(c)**) it was gently sloping.

In FR-grown cells, larger size 645–660 nm peak was attended with smaller 715–725 nm peak (**Figures 2(d)** and **3(d)**). Modified emission spectra, as compared with WL-grown cells, could be explained by some changes in PBS arrangement and behavior during the FaRLiP response [45, 48, 49].

The comparison of emission spectra in **Figures 2** and **3** showed that, in the case of FRL-grown cells, direct excitation of chlorophylls (blue light excitation, 440-nm

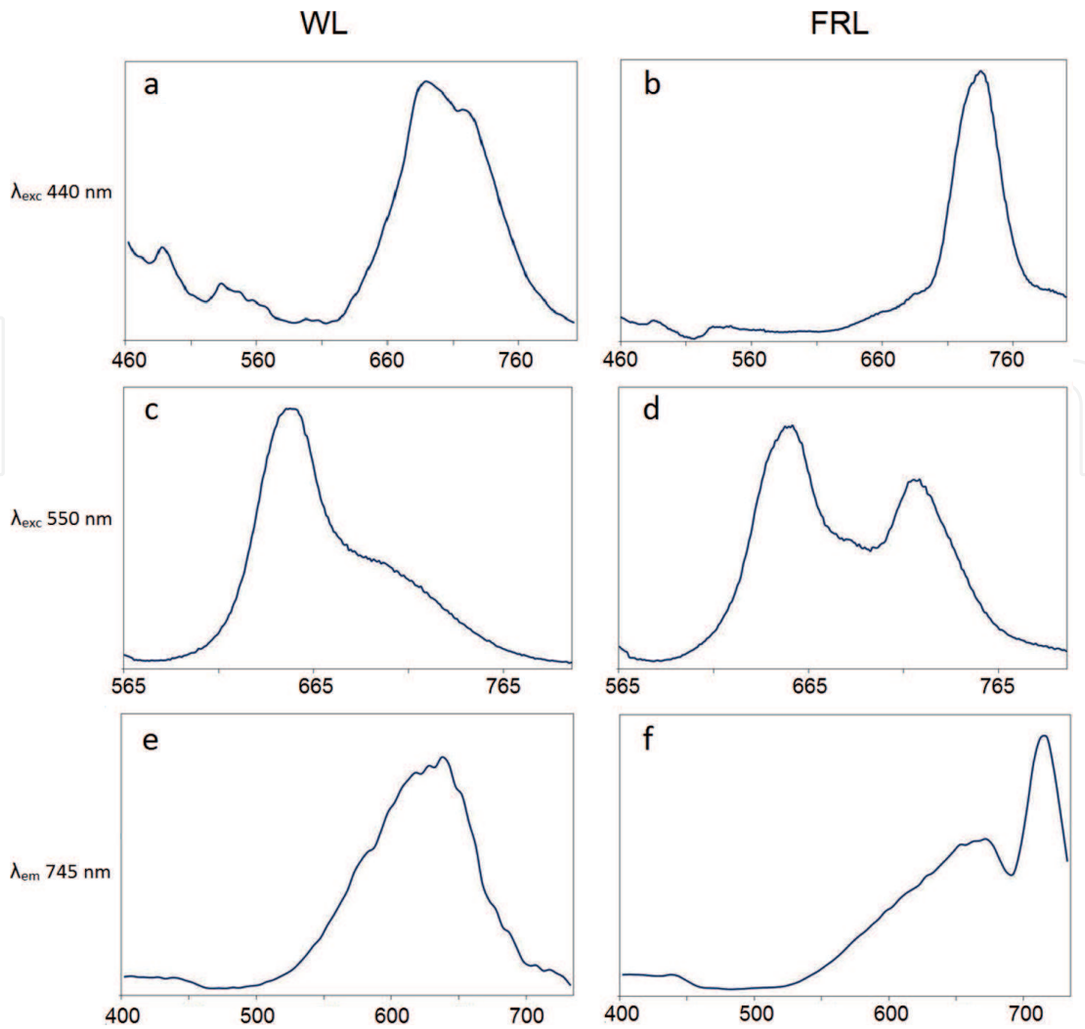


Figure 2.
Fluorescence spectra of white light (WL)-grown (a, c) or far-red light (FRL)-grown (b, d) Chlorogloeopsis *sp. CALU 759 cells. Emission spectra: 440 nm (a, b) and 550 nm (c, d) excitation. Excitation spectra: chlorophyll fluorescence at 745 nm (e, f).*

wavelength) was more efficient than via antenna PBP pigments (550-nm green light exciting mainly PE and PC). This effect can be explained by PBS uncoupling with PSII because bulk fluorescence at room temperature is known to issue from PSII. If not coupled, PBP excited at 550 nm should exhibit considerable fluorescence around 700 nm (that is the case here).

Fluorescence excitation spectra of WL-grown cells (**Figures 2(e)** and **3(e)**) demonstrated a single peak at 625–650 nm excitation wavelength. Negligible fluorescence during illumination with 400–500 nm light (which preferentially excited chlorophylls) can be explained by shading of the blue region with photosynthetically inactive carotenoids. At the same time, fluorescence during illumination with ~600 nm (which preferentially excited PBP) raised a maximum chlorophyll fluorescence that additionally indicated an efficient coupling of PBS with PSII. In contrast to WL-grown cells, in FRL-grown cells (**Figures 2(f)** and **3(f)**), peak chlorophyll fluorescence was observed at ~670 and ~ 720 nm excitation. High ratio of 720-nm peak/670-nm peak size additionally witnesses for a change of photosynthetic apparatus at FaRLiP response. It is noteworthy that unlike cryogenic method, room temperature fluorescence detection could not comment on the specificity of Chl *f* functioning in analyzed strains (that is the aim of our future research).

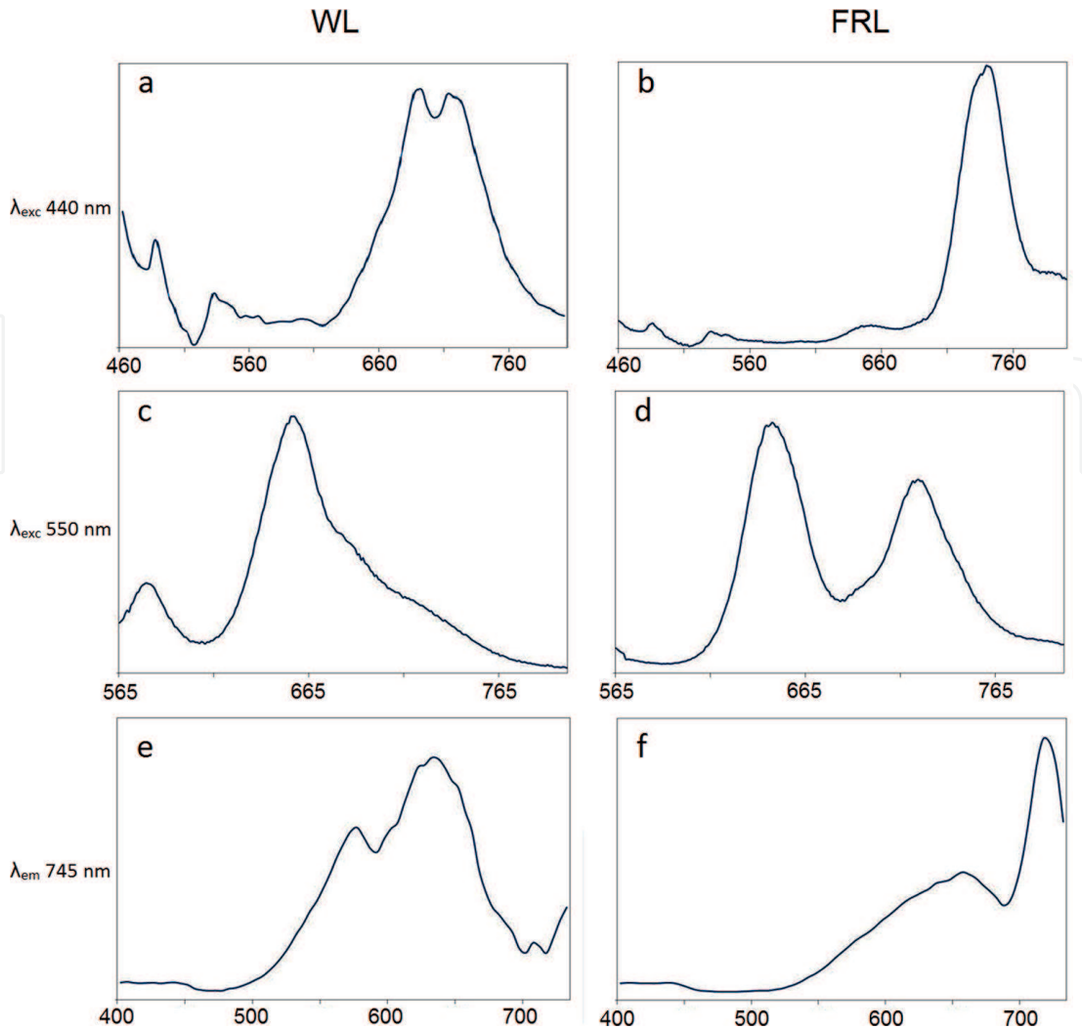


Figure 3.
Fluorescence spectra of white light (WL)-grown (a, c) or far-red light (FRL)-grown (b, d) Synechocystis *sp. CALU 1173 cells. Emission spectra: 440 nm (a, b) and 550 nm (c, d) excitation. Excitation spectra: Chlorophyll fluorescence at 745 nm (e, f).*

5.5 CLSM of chlorophylls and phycobiliproteins in white light- and far-red light-grown cells

In the case of WL-grown *Chlorogloeopsis* sp. CALU 759 (**Figure 4**), false-green 670–700 nm fluorescence typical for Chl *a* (**Figure 4(a)**) and false-blue 620–650 nm fluorescence typical for PC (**Figure 4(b)**) were observed not only at

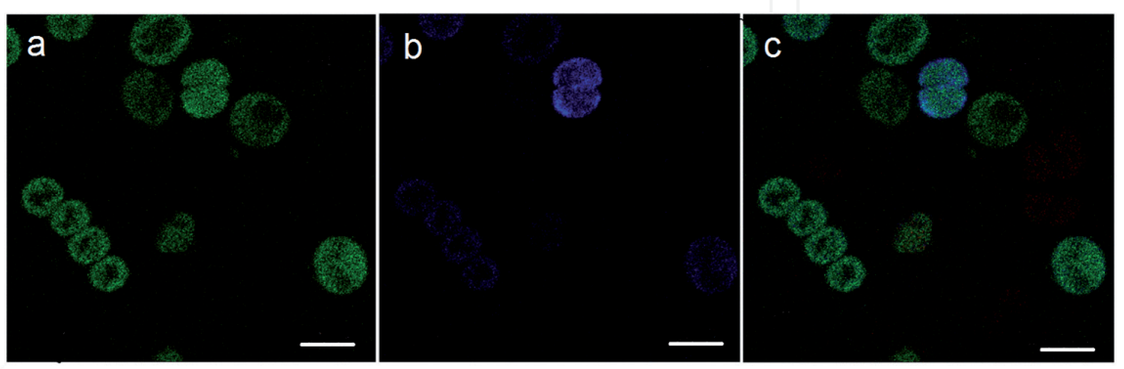


Figure 4.
Laser confocal scanning micrographs of white light-grown Chlorogloeopsis *sp. CALU 759 cells. Chlorophyll* a *fluorescence is shown with false-green (a); phycocyanin fluorescence is shown with false-blue (b); chlorophyll* a *and phycocyanin total fluorescence (c).*

cell periphery but also in cell center. Moreover, mutually overlapping fluorescence channels (**Figure 4(c)**) indicated that the pigments had a common localization.

Similar topology was observed in FRL-grown *Chlorogloeopsis* sp. CALU 759 (**Figure 5**). Importantly, Chl *a* false-green emission (**Figure 5(a)**), Chl *f*

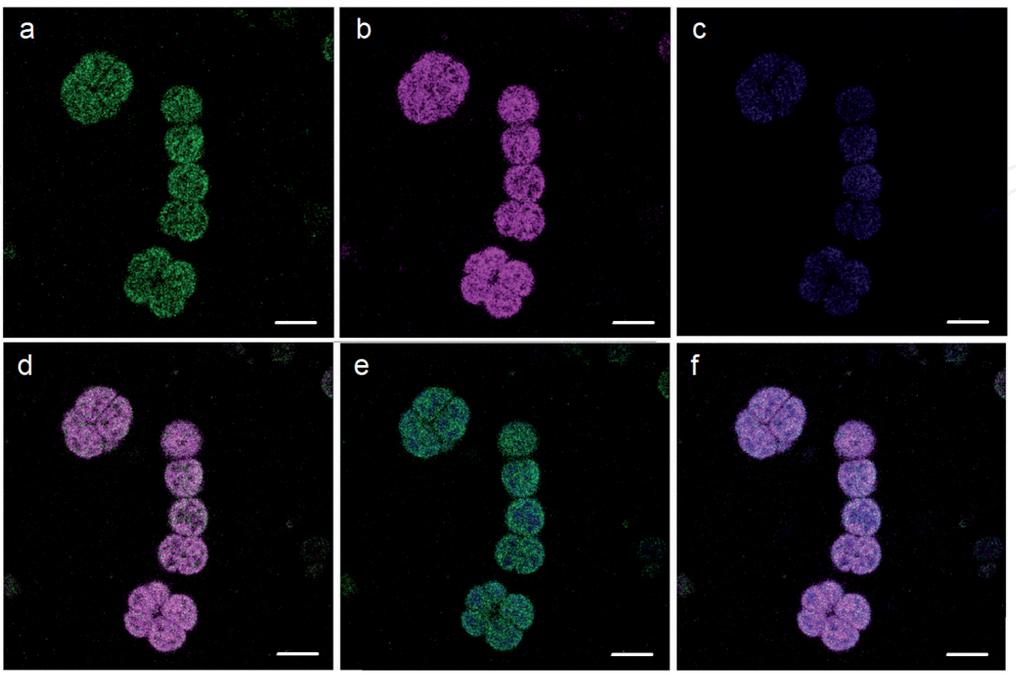


Figure 5.
Laser confocal scanning micrographs of far-red light-grown Chlorogloeopsis *sp. CALU 759 cells. Chlorophyll* a *fluorescence is shown with false-green (a); chlorophyll* f *fluorescence is shown with false-purple (b); phycocyanin fluorescence is shown with false-blue (c); chlorophyll* a *and chlorophyll* f *fluorescence (d); chlorophyll* a *and phycocyanin fluorescence (e); total pigment fluorescence (f). Scale bar, 5 μm.*

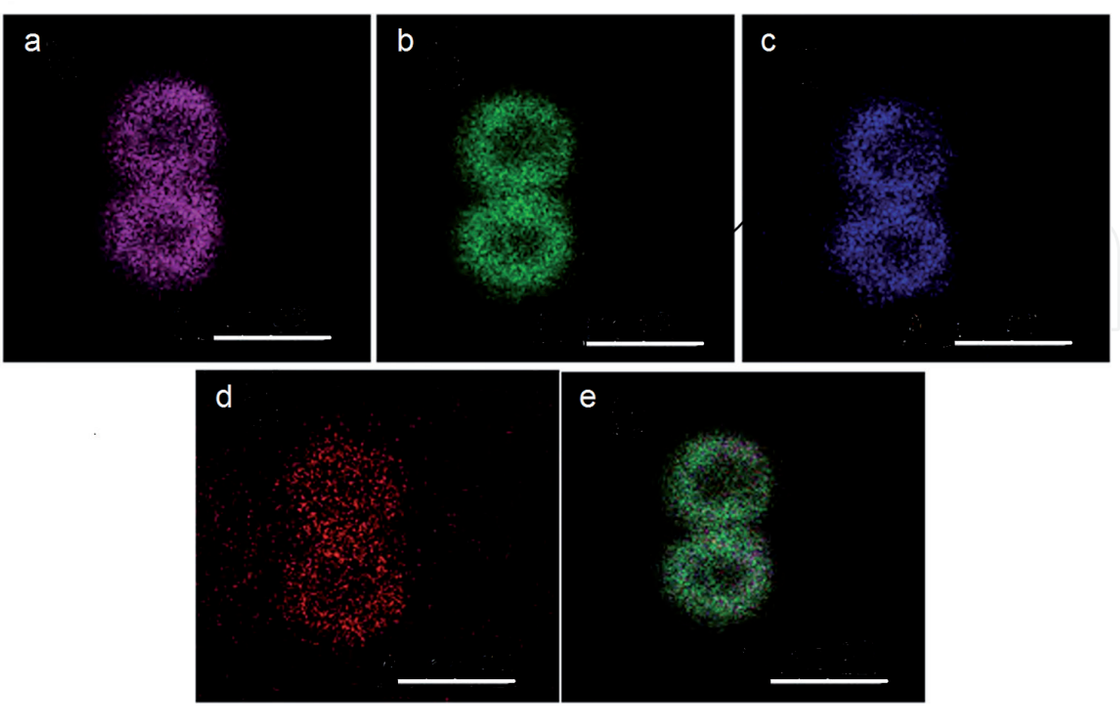


Figure 6.
Laser confocal scanning micrographs of far-red light-grown Synechocystis *sp. CALU 1173 cells. Chlorophyll f fluorescence is shown with false-purple (a); chlorophyll a fluorescence is shown with false-green (b); phycocyanin fluorescence is shown with false-blue (c); phycoerythrin fluorescence is shown with false-red (d); total pigment fluorescence (e). Scale bar, 2 μm.*

false-purple emission (**Figure 5(b)**), and Chl *a*/Chl *f* mixed emission (**Figure 5(d)**) coincided spatially, and that indicated a relative integrity of photosynthetic apparatus. At the same time, PC fluorescence showed a more homogeneous distribution (**Figure 5(c,e,f)**). Thus, PBS either partially detached from thylakoid membrane, or PBS coupling with PSII lowered (which is in agreement with steady-state fluorescence results). Similar images were obtained for FRL-grown *Synechococcus* sp. PCC 7335 [67].

In the case of FRL-grown *Synechocystis* sp. CALU 1173 (**Figure 6**), fluorescence topology was similar within the observed wavelength span. Namely, Chl *f* false-purple fluorescence (**Figure 6(a)**), Chl *a* false-green fluorescence (**Figure 6(b)**), PC false-blue fluorescence (**Figure 6(c)**), PE false-red fluorescence (**Figure 6(d)**), and pigment total fluorescence (**Figure 6(e)**) occupied cell periphery, and fluorescence channels mutually overlapped. The observed fluorescence topology matched with the electron microscopy data on peripheral thylakoid arrangement in *Synechocystis* spp. [69, 70].

6. Conclusion

Over past decades, FaRLiP photoacclimation has been studied in many respects, although in a small number of cyanobacterial strains [3]. In this connection, novel Chl *f*-producing strains *Chlorogloeopsis* sp. CALU 759 and *Synechocystis* sp. CALU 1173 would represent promising model objects. Importantly, although they belong to alternative morphotypes (trichome and single cell, respectively) and two distant phylogenetic lineages [71], fluorescence patterns of their FRL-grown cells similarly fall within the general FaRLiP response.

Acknowledgements

The authors are grateful to St. Petersburg University Research Center "Cultivation of microorganisms" (http://researchpark.spbu.ru/collection-ccem-rus/1628-ccem-kollekciya-calu-rus) for a help with strains maintenance. They also thank St. Petersburg University Research Centers "Molecular and Cell Technologies" and "Chromas" for research fellowship. The work was supported by the Russian Foundation for Fundamental Research, project no. 20-04-00020.

DOI: http://dx.doi.org/10.5772/intechopen.92776

IntechOpen

IntechOpen

Author details

Svetlana Averina*, Ekaterina Senatskaya and Alexander Pinevich
Saint-Petersburg State University, St. Petersburg, Russia

*Address all correspondence to: s.averina@spbu.ru; spbu.svetik@rambler.ru

IntechOpen

© 2020 The Author(s). Licensee IntechOpen. Distributed under the terms of the Creative Commons Attribution - NonCommercial 4.0 License (https://creativecommons.org/licenses/by-nc/4.0/), which permits use, distribution and reproduction for non-commercial purposes, provided the original is properly cited. BY–NC

References

[1] Miyashita H, Ikemoto H, Kurano N, et al. Chlorophyll *d* as a major pigment. Nature. 1996;**383**:402. DOI: 10.1038.383402a0

[2] Gan F, Bryant DA. Adaptive and acclimative responses of cyanobacteria to far-red light. Environmental Microbiology. 2015;**17**:3450-3465. DOI: 0.1111/1462-2920.12992

[3] Averina S, Velichko N, Senatskaya E, Pinevich A. Far-red light photoadaptations in aquatic cyanobacteria. Hydrobiologia. 2018;**813**:1-17. DOI: 10.1007/s10750-018-3519-x

[4] Pinevich A, Velichko N, Ivanikova N. Cyanobacteria of the genus *Prochlorothrix*. Frontiers in Microbiology. 2012;**3**:173. DOI: 10.3389/fmicb.2012.00173

[5] Averina S, Velichko N, Senatskaya E, et al. Non *a*-chlorophylls in cyanbacteria. Photosynthetica. 2019;**57**:1109-1118. DOI: 10.32615/ps.2019.130

[6] Adir N. Elucidation of the molecular structures of components of the phycobilisome: Reconstructing a giant. Photosynthesis Research. 2005;**85**:15-32. DOI: 10.1007/s11120-004-2143-y

[7] Watanabe M, Ikeuchi M. Phycobilisome: Architecture of a light-harvesting supercomplex. Photosynthesis Research. 2013;**116**:265-276. DOI: 10.1007/s11120-013-9905-3

[8] MacColl R. Cyanobacterial phycobilisomes. Journal of Structural Biology. 1998;**124**:311-334. DOI: 10.1006/jsbi.1998.4062

[9] Scheer H, Zhao KH. Biliprotein maturation: The chromophore attachment. Molecular Microbiology. 2008;**68**:263-276. DOI: 10.1111/j.1365-2958.2008.06160.x

[10] Chang L, Liu X, Li Y, et al. Structural organization of an intact phycobilisome and its association with photosystem II. Cell Research. 2015;**25**:726-737. DOI: 10.1038/cr.2015.59

[11] Zhang J, Ma J, Liu D, et al. Structure of phycobilisome from the red alga *Griffithsia pacifica*. Nature. 2017;**551**:57-63. DOI: 10.1038/nature24278

[12] Muramatsu M, Hihara Y. Acclimation to high-light conditions in cyanobacteria: From gene expression to physiological responses. Journal of Plant Research. 2012;**125**:11-39. DOI: 10.1007/s10265-011-0454-6

[13] Mullineaux CW. Electron transport and light-harvesting switches in cyanobacteria. Frontiers in Plant Science. 2014;**5**:7. DOI: 10.3389/fpls.2014.00007

[14] McConnell MD, Koop R, Vasil'ev S, Bruce D. Regulation of the distribution of chlorophyll and phycobilin-absorbed energy in cyanobacteria. A structure-based model for the light state transition. Plant Physiology. 2002;**130**:1201-1212. DOI: 10.1104/pp.009845

[15] Mullineaux CW, Allen JF. State 1-state 2 transitions in the cyanobacterium *Synechococcus* 6301 are controlled by the redox state of electron carriers between photosystem I and II. Photosynthesis Research. 1990;**23**:297-311. DOI: 10.1007/BF00034860

[16] Hirose Y, Chihong S, Watanabe M, et al. Diverse chromatic acclimation processes regulating phycoerythrocyanin and rod-shaped phycobilisome in cyanobacteria.

Molecular Plant. 2019;**12**:715-725. DOI: 0.1016/jmolp.2019.02.010

[17] Sanfilippo JE, Garczarek L, Partensky F, Kehoe DM. Chromatic acclimation in cyanobacteria: A diverse and widespread process for optimizing photosynthesis. Annual Review of Microbiology. 2019;**73**:407-433. DOI: 10.1146/annurev-micro-020518-115738

[18] Tandeau de Marsac N. Occurrence and nature of chromatic adaptation in cyanobacteria. Journal of Bacteriology. 1977;**130**:82-91. PMCID: PMC235176

[19] Yoshihara S, Katayama M, Geng X, Ikeuchi M. Cyanobacterial phytochrome-like PixJ1 holoprotein shows novel reversible photoconversion between blue- and green-absorbing forms. Plant & Cell Physiology. 2004;**45**:1729-1737. DOI: 10.1093/pcp/pch214

[20] Ikeuchi M, Ishizuka T. Cyanobacteriochromes: A new superfamily of tetrapyrrole-binding photoreceptors in cyanobacteria. Photochemical & Photobiological Sciences. 2008;**7**:1159-1167. DOI: 10.1039/B802660M

[21] Rockwell NC, Lagarias JC. A brief history of phytochromes. ChemPhysChem. 2010;**11**:1172-1180. DOI: 10.1002/cphc.2009200900894

[22] Hirose Y, Shimada T, Narikawa R, et al. Cyanobacteriochrome CcaS is the green light receptor that induces the expression of phycobilisome linker protein. Proceedings of the National Academy of Sciences of the United States of America. 2008;**105**:9528-9533. DOI: 10.1073/pnas.0801826105

[23] Hirose Y, Rockwell NC, Nishiyama K, et al. Green/red cyanobacteriochromes regulate complementary chromatic acclimation via a protochromic photocycle. Proceedings of the National Academy of Sciences of the United States of America. 2013;**110**:4974-4979. DOI: 10.1073/pnas.1302909110

[24] Kehoe DM, Grossman AR. Similarity of a chromatic adaptation sensor to phytochrome and ethylene receptors. Science. 1996;**273**:1409-1412. DOI: 10.1126/science.273.5280.1409

[25] Everroad C, Six C, Partensky F, et al. Biochemical bases of type IV chromatic adaptation in marine *Synechococcus* spp. Journal of Bacteriology. 2006;**188**:3345-3356. DOI: 10.1128/JB.188.9.3345-3356.2006

[26] Shukla A, Biswas A, Blot N, et al. Phycoerythrin-specific bilin lyase-isomerase controls blue-green chromatic acclimation in marine *Synechococcus*. Proceedings of the National Academy of Sciences of the United States of America. 2012;**109**:20136-20141. DOI: 10.1073/pnas.1211777109

[27] Grebert T, Dore H, Partensky F, et al. Light color acclimation is a key process in the global ocean distribution of *Synechococcus* cyanobacteria. Proceedings of the National Academy of Sciences of the United States of America. 2018;**115**:E2010-E2019. DOI: 10.1073/pnas.1717069115

[28] Sanfilippo JE, Nguyen AA, Karty JA, et al. Self-regulating genomic island encoding tandem regulators confers chromatic acclimation to marine *Synechococcus*. Proceedings of the National Academy of Sciences of the United States of America. 2016;**113**:6077-6082. DOI: 10.1073/pnas.1600625113

[29] Chen M, Floetenmeyer M, Bibby TS. Supramolecular organization of phycobiliproteins in the chlorophyll *d*-containing cyanobacterium *Acaryochloris marina*. FEBS Letters. 2009;**583**:2535-2539. DOI: 10.1016/j.febslett.2009.07.012

[30] Hu Q, Marquardt J, Iwasaki I, et al. Molecular structure, localization and function of biliproteins in the chlorophyll *a/d* containing oxygenic photosynthetic prokaryote *Acaryochloris marina*. Biochimica et Biophysica Acta - Bioenergetics. 1999;**1412**:250-261. DOI: 10.1016/S0005-2728(99)0067-5

[31] Gloag RS, Ritchie RJ, Chen M, et al. Chromatic photoacclimation, photosynthetic electron transport and oxygen evolution in the chlorophyll *d*-containing oxyphotobacterium *Acaryochloris marina*. Biochimica et Biophysica Acta - Bioenergetics. 2007;**1767**:127-135. DOI: 10.1007/s11120-009-9466

[32] Duxbury Z, Schliep M, Ritchie RJ, et al. Chromatic photoacclimation extends utilisable photosynthetically active radiation in the chlorophyll *d*-containing cyanobacterium, *Acaryochloris marina*. Photosynthesis Research. 2009;**101**:69-75. DOI: 10.1007/s11120-009-9466-7

[33] Loughlin PC, Duxbury Z, Mugerwa TTM, et al. Spectral properties of bacteriophytochrome AM15894 in the chlorophyll *d*-containing cyanobacterium *Acaryochloris marina*. Scientific Reports. 2016;**6**:27547. DOI: 10.1038/srep27547

[34] Kondo K, Geng XX, Katayama M, Ikeuchi M. Distinct roles of CpcG1 and CpcG2 in phycobilisome assembly in the cyanobacterium *Synechocystis* sp PCC 6803. Photosynthesis Research. 2005;**84**:269-273. DOI: 10.1007/s11120-004-7762-9

[35] Chen M, Li Y, Birch D, Willows RD. A cyanobacterium that contains chlorophyll *f*—A red-absorbing photopigment. FEBS Letters. 2012;**586**:3249-3254. DOI: 10.1016/j.febslett.2012.06.045

[36] Miyashita H, Adachi K, Kurano N, et al. Pigment composition of a novel oxygenic photosynthetic prokaryote containing chlorophyll *d* as the major chlorophyll. Plant & Cell Physiology. 1997;**38**:274-281. DOI: 0.1093/oxfordjournals.pcp.a029163

[37] Schiller H, Senger H, Miyashita H, et al. Light-harvesting in *Acaryochloris marina*: Spectroscopic characterization of a chlorophyll *d*-dominated photosynthetic antenna system. FEBS Letters. 1997;**410**:433-436. DOI: 10.1016/s0014-05793(97)00620-0

[38] Mimuro M, Akimoto S, Gotoh T, et al. Identification of the primary electron donor in PS II of the Chl *d* dominated cyanobacterium *Acaryochloris marina*. FEBS Letters. 2004;**556**:95-98. DOI: 10.1016/s0014-5793(03)-01383-8

[39] Lin Y, Crossett B, Chen M. Effects of anaerobic conditions on photosynthetic units of *Acaryochloris marina*. In: Proceedings of 15th International Conference on Photosynthesis. Berlin, Heidelberg: Springer Science + Business Media B.V.; 2013. pp. 121-124. DOI: 10.1007/978-3-642-32034-7_26

[40] Hu Q, Miyashita H, Iwasaki I, et al. A photosystem I reaction center driven by chlorophyll *d* in oxygenic photosynthesis. Proceedings of the National Academy of Sciences of the United States of America. 1998;**95**:13319-13323. DOI: 10.1073/pnas.95.22.13319

[41] Tomo T, Shinoda T, Chen M, et al. Energy transfer processes in chlorophyll *f*-containing cyanobacteria using time-resolved fluorescence spectroscopy on intact cells. Biochimica et Biophysica Acta - Bioenergetics. 2014;**1837**:1484-1489. DOI: 10.1016/jbbabio.2014.04.009

[42] Chen M, Hiller RG, Howe CJ, Larkum AWD. Unique origin and lateral transfer of prokaryotic chlorophyll-*b* and chlorophyll-*d* light-harvesting systems. Molecular Biology and

Evolution. 2005;**22**:21-28. DOI: 10.1093/molbev/msh250

[43] Chen M, Telfer A, Lin S, et al. The nature of the photosystem II reaction centre in the chlorophyll *d*-containing prokaryote, *Acaryochloris marina*. Photochemical & Photobiological Sciences. 2005;**4**:1060-1064. DOI: 10.1039/b507057k

[44] Akutsu S, Fujinuma D, Furukawa H, et al. Pigment analysis of a chlorophyll *f*-containing cyanobacterium strain KC1 isolated from Lake Biwa. Photomedicine and Photobiology. 2011;**33**:35-40

[45] Gan F, Zhang S, Rockwell NC, et al. Extensive remodeling of a cyanobacterial photosynthetic apparatus in far-red light. Science. 2014;**345**:1312-1317. DOI: 10.1126/science.1256963

[46] Gan F, Shen G, Bryant DA. Occurrence of far-red light photoacclimation (FaRLiP) in diverse cyanobacteria. Life. 2015;**5**:4-24. DOI: 10.3390/life501004

[47] Zhao C, Gan F, Shen G, Bryant DA. RfpA, RfpB and RfpC are the master control elements of far-red light photoacclimation (FaRLiP). Frontiers in Microbiology. 2015;**6**:1303. DOI: 10.3389/fmicb.2015.01303

[48] Li Y, Lin Y, Garvey CJ, et al. Characterization of red-shifted phycobilisomes isolated from the chlorophyll *f*-containing cyanobacterium *Halomicronema hongdechloris*. Biochimica et Biophysica Acta - Bioenergetics. 2016;**1857**:107-114. DOI: 10.1016/j.bbabio.2015.10.009

[49] Ho M-Y, Gan F, Shen G, Bryant DA. Far-red light photoacclimation (FaRLiP) in *Synechococcus* sp. PCC 7335. II. Characterization of phycobiliproteins produced during acclimation to far-red light. Photosynthesis Research. 2016;**131**:187-202. DOI: 10.1007/s11120-016-0303-6

[50] Ho M-Y, Gan F, Shen G, et al. Far-red light photoacclimation (FaRLiP) in *Synechococcus* sp. PCC 7335: I. Regulation of FaRLiP gene expression. Photosynthesis Research. 2016;**131**:173-186. DOI: 1o.1007/s11120-016-0309-z

[51] Lamb JJ, Røkke G, Hohmann-Marriott MF. Chlorophyll fluorescence emission spectroscopy of oxygenic organisms at 77 K. Photosynthetica. 2018;**56**:105-124. DOI: 10.1007/s11099-018-0791-y

[52] Cho F, Govindjee. Low-temperature (4-77°K) spectroscopy of *Anacystis*; temperature dependence of energy transfer efficiency. Biochimica et Biophysica Acta. 1970;**216**:151-161. DOI: 10.1016/0005-2728(70)90167-2

[53] Govindjee, Shevela D, Björn LO. Evolution of the Z-scheme of photosynthesis: A perspective. Photosynthesis Research. 2017;**133**:5-15. DOI: 10.1007/s11120-016-0333-z

[54] Akimoto S, Shinoda T, Chen M, Allakhverdiev SI, Tomo T. Energy transfer in the chlorophyll *f*-containing cyanobacterium, *Halomicronema hongdechloris*, analyzed by time-resolved fluorescence spectroscopies. Photosynthesis Research. 2015;**125**:115-122. DOI: 10.1007/s11120-015-0091-3

[55] Ho M-Y, Niedzwiedzki DM, MacGregor-Chatwin C, et al. Extensive remodeling of the photosynthetic apparatus alters energy transfer among photosynthetic complexes when cyanobacteria acclimate to far-red light. Biochimica et Biophysica Acta - Bioenergetics. 2020;**1861**:148064. DOI: 10.1016/j.bbabio.2019.148064

[56] Millar DP. Time-resolved fluorescence spectroscopy. Current Opinion in Structural Biology.

1996;**6**:637-642. DOI: 10.1016/s0959-440x(96)80030-3

[57] Chukhutsina VU, Holzwarth AR, Croce R. Time-resolved fluorescence measurements on leaves: Principles and recent developments. Photosynthesis Research. 2019;**140**:355-369. DOI: 10.1007/s11120-018-0607-8

[58] Schmitt FJ, Campbell ZY, Mai V, et al. Photosynthesis supported by a chlorophyll *f*-dependent, entropy-driven uphill energy transfer in *Halomicronema hongdechloris* cells adapted to far-red light. Photosynthesis Research. 2019;**139**:185-201. DOI: 10.1007/s11120-018-0556-2

[59] Kaucikas M, Nürnberg D, Dorlhiac G, et al. Femtosecond visible transient absorption spectroscopy of chlorophyll *f*-containing photosystem I. Biophysical Journal. 2017;**112**:234-249. DOI: 10.1016/j.bpj.201612.022

[60] Nürnberg DJ, Morton J, Santabarbara S, et al. Photochemistry beyond the red-limit in chlorophyll *f*-photosystems. Science. 2018;**360**: 1210-1213. DOI: 10.1026/science.aar8313

[61] Itoh S, Ohno T, Noji T, et al. Harvesting far-red light by chlorophyll *f* in photosystems I and II of unicellular cyanobacterium strain KC1. Plant & Cell Physiology. 2015;**56**:2024-2034. DOI: 10.1039/pcp/pcv122

[62] Cherepanov DA, Shelaev IV, Gostev FE, et al. Evidence that chlorophyll *f* functions solely as an antenna pigment in far-red-light photosystem I from *Fischerella thermalis* PCC 7521. Biochimica et Biophysica Acta - Bioenergetics. 2020;**1861**:148-184. DOI: 10.1016/j.bbabio.2020.148184

[63] Bar-Zvi S, Lahav A, Harris D, et al. Structural heterogeneity leads to functional homogeneity in *A. marina* phycocyanin. Biochimica et Biophysica Acta - Bioenergetics. 2018;**1859**:544-553. DOI: 10.1016/j.bbabio.2018.04.007

[64] Krause GH, Weis E. Chlorophyll fluorescence and photosynthesis: The basics. Annual Review of Plant Physiology and Plant Molecular Biology. 1991;**42**:313-349. DOI: 10.1146/annurev.pp.42.060191.001525

[65] López-Legentil S, Song B, Bosch M, et al. Cyanobacterial diversity and a new *Acaryochloris*-like symbiont from Bahamian sea-squirts. PLoS One. 2011;**6**:e23938. DOI: 10.1371/journal.pone.0023938

[66] Martinez-Garcia M, Koblizek M, Lopez-Legentil S, Anton J. Epibiosis of oxygenic phototrophs containing chlorophylls *a*, *b*, *c* and *d* on the colonial ascidian *Cystodytes dellechiajei*. Microbial Ecology. 2011;**61**:13-19. DOI: 10.1007/s00248-010-9694-6

[67] Majumder EL-W, Wolf BM, Liu H, et al. Subcellular pigment distribution is altered under far-red light acclimation in cyanobacteria that contain chlorophyll *f*. Photosynthesis Research. 2017;**134**:183-192. DOI: 10.1007/s11120-017-0428-1

[68] Pinevich AV, Matthijs HCP, Gavrilova OV, et al. New ultrastructural aspects of membranes and cell inclusions in *Prochlorothrix hollandica* (*Prochlorales*, *Cyanobacteria*). Microbios. 1996;**84**:217-225

[69] Korelusova J, Kaštovsky J, Komarek J. Heterogeneity of the cyanobacterial genus *Synechocystis* and description of a new genus, *Geminocystis*. Journal of Phycology. 2009;**45**:928-937. DOI: 10.1111/j.1529-8817.2009.00701.x

[70] Komarek J, Kaštovsky J, Mareš J, Johansen JR. Taxonomic classification of cyanoprokaryotes (cyanobacterial genera) using a polyphasic approach. Preslia. 2014;**86**:295-335

[71] Castenholz RW. General characterization of cyanobacteria. In: Boone DR, Castenholz RW, editors. Bergey's Manual of Systematic Bacteriology. New York: Springer-Verlag; 2001. pp. 474-487

IntechOpen

IntechOpen